RESEARCH ARTICLE

Gallic acid, a histone acetyltransferase inhibitor, suppresses β-amyloid neurotoxicity by inhibiting microglial-mediated neuroinflammation

Mi-Jeong Kim[1], Ah-Reum Seong[1], Jung-Yoon Yoo[1], Cheng-Hao Jin[1], Yoo-Hyun Lee[2], Young Jun Kim[3], Jeongmin Lee[4], Woo Jin Jun[5] and Ho-Geun Yoon[1]

[1] Department of Biochemistry and Molecular Biology, Yonsei University College of Medicine, Seoul, Korea
[2] Department of Food Science and Nutrition, The University of Suwon, Kyunggi-do, Korea
[3] Department of Food and Biotechnology, Korea University, Chungnam, South Korea
[4] Department of Medical Nutrition, Kyung Hee University, Kyunggi-do, South Korea
[5] Department of Food and Nutrition, Chonnam National University, Gwangju, South Korea

Received: April 19, 2011
Revised: August 16, 2011
Accepted: September 2, 2011

Scope: We examined the biological effect of gallic acid (GA) as a nuclear factor (NF)-κB acetyltransferase inhibitor on microglial-mediated β-amyloid neurotoxicity and restorative effects on the Aβ-induced cognitive dysfunction.

Methods and results: The protective effects of GA on the survival of neuronal cells were assessed with an MTT assay and a co-culture system. For the co-culture experiments, both BV-2 and primary microglia cells were treated with GA prior to Aβ stimulation, and conditioned media were transferred to Neuro-2A cells. The mRNA and protein levels of inflammatory cytokines in both microglia and Neuro-2A cells were assessed with real-time polymerase chain reaction and western blotting. Inhibition of nuclear factor kappa B (NF-κB) acetylation with GA treatment resulted in reduced cytokine production in microglia cells and protection of neuronal cells from Aβ-induced neurotoxicity. Furthermore, we observed a restorative effect of GA on Aβ-induced cognitive dysfunction in mice with Y-maze and passive avoidance tests. Finally, we found that GA treatment efficiently blocked neuronal cell death by downregulating the expression of cytokines and the in vivo levels of NF-κB acetylation.

Conclusion: These results suggest that selective inhibition of NF-κB acetylation by the histone acetyltransferase inhibitor GA is a possible therapeutic approach for alleviating the inflammatory progression of Alzheimer disease.

Keywords:
Alzheimer disease / Gallic acid / Histone acetyltransferase inhibitor / Microglia / Neuroinflammation

1 Introduction

Alzheimer disease (AD) is the most common form of dementia and is characterized by progressive impairment of cognitive function and behavior [1]. The pathological features of AD are the accumulation of senile plaques containing amyloid beta (Aβ) peptide cores and neurofibrillary tangles containing hyperphosphorylated tau protein. According to several studies, Aβ peptide aggregation occurs frequently in the brains of patients with AD, and fibrillary Aβ aggregates induce neurotoxicity [2]. Normally, microglial

Correspondence: Dr. Ho-Geun Yoon, Yonsei University College of Medicine, 134 Shinchon-dong, Seodaemun-gu, Seoul, Korea
E-mail: yhgeun@yuhs.ac
Fax: +82-2-312-5041

Abbreviations: Aβ, β-amyloid; **AD,** Alzheimer disease; **B.W.,** body weight; **CBP,** CREB-binding protein; **CM,** conditioned media; **COX-2,** cyclooxygenase-2; **CNS,** central nervous system; **GA,** gallic acid; **HAT,** histone acetyltransferase; **HATi,** HAT inhibitor; **iNOS,** inducible nitric oxide synthase; **MTT,** 3-(4,5-dimethylthiazol-2-ly)-2,5-diphenyl tetrazolium bromide; **NF-κB,** nuclear factor-κB; **PCAF,** p300/CBP-associated factor; **STL,** step-through latency; **TNF-α,** tumour necrosis factor alpha

cells play neurotrophic roles in immune and inflammatory responses in the central nervous system (CNS). They are activated during neuropathological conditions to restore CNS homeostasis [3]. However, the abnormal activation of microglia promotes neuronal injury through the release of pro-inflammatory and cytotoxic factors, including tumor necrosis factor alpha (TNF-α), IL-1β, inducible nitric oxide synthase (iNOS), cyclooxygenase-2 (COX-2), nitric oxide, and reactive oxygen species that contribute to localized or more widespread CNS injury [4]. Aggregated Aβ peptides induce activation of microglia [5]. In addition, amyloid-dependent activation of microglia results in acquisition of a reactive phenotype and secretion of proinflammatory molecules [6, 7]. Therefore, blocking Aβ-induced activation of microglia may be a therapeutic approach for alleviating the progression of AD.

Activation of the immune system and inflammatory responses is regulated by transcription factors, especially nuclear factor kappa B (NF-κB) [8]. The NF-κB signaling pathway is evolutionarily conserved. In mammals, five Rel family members have been identified: RelA/p65, RelB, c-RelA, p50/p105, and p52/p100 [9, 10]. NF-κB has also been shown to control the induction of transcription of pro-inflammatory mediators such as COX-2, iNOS, TNF-α, IL-1β, and IL-6 [11]. For nuclear translocation, RelA is acetylated by histone acetyltransferase (HAT) enzymes including p300/CREB-binding protein (CBP) and p300/CBP-associated factor (PCAF) [12, 13]. Deacetylation of p65 promotes its effective binding to IκBα and leads to IκBα-dependent nuclear export of the NFκB complex via a chromosomal region maintenance 1-dependent pathway [12]. Reversible acetylation of p65 thus functions as a molecular switch that controls the duration of the NF-κB transcriptional response [14]. Because NF-κB is a member of a ubiquitously expressed family of transcription factors that control the expression of important genes involved in inflammatory and immune responses and cellular proliferation, it is not surprising that NF-κB is involved in numerous and diverse diseases including the neuronal death induced by Aβ [15, 16, 17]. In AD brains, RelA/p65 immunoreactivity is stronger in neurons, astrocytes, and microglial cells surrounding amyloid plaques [18]. Interestingly, it has been also proposed that NF-κB activation in Aβ-induced microglia is directly correlated with the pathogenic events of AD [18]. Therefore, RelA acetylation is an interesting target for inhibiting NF-κB-mediated inflammation, which is involved in chronic inflammation and disease.

During the last 5 years, several compounds have been reported to inhibit HATs [19–23]. Garcinol inhibits p300 and PCAF in vitro and in vivo, anacardic acid inhibits TIP60, p300, and PCAF, curcumin inhibits p300 and PCAF, procyanidin B3 inhibits p300 and TIP60, and both epigallocatechin gallate and gallic acid (GA) inhibit HAT enzymes with a broad enzyme specificity [19–23]. Although epigenetic modulators such as histone deacetylase inhibitors and DNA methyltransferases are currently in clinical trials, there is little information on the link between the inhibition of catalytic HAT function and the biological effects.

GA (3,4,5-trihydroxybenzoic acid) is a major compound found in gallnuts, sumac, witch hazel, tea leaves, oak bark, and other plants [24]. GA and its derivatives are natural polyphenols; these compounds are particularly abundant in processed beverages such as red wine and green tea [25]. Recently, the diverse biological activities of GA, including antioxidant, anti-inflammatory, antimicrobial, and anti-allergic activities, have been demonstrated [26]. Among them, grape seed extract containing GA, catechin, epigallocatechin gallate, and proanthocyanidin was shown to prevent Aβ deposition and attenuate inflammation in the brain of an AD mouse [27]. In this regard, we recently reported that GA possesses potent anti-HAT activity and inhibits RelA acetylation by directly inhibiting the activity of HAT enzymes, which finally leads to downregulation of NF-κB function via diverse inflammatory signals [22]. Thus, GA may be a potential neuroprotective agent; however, the in vivo effects of GA on Aβ-mediated neurotoxicity have not been examined.

In this study, we examined the biological effect of the HAT inhibitor (HATi), GA, on Aβ-induced neuroinflammation and neuronal cell death, which were triggered by activated microglia. Using co-culture analysis, we show that GA efficiently suppressed Aβ-induced cytokine production in microglia by inhibiting RelA acetylation, preventing neuronal cell death caused by Aβ-induced neurotoxicity. Furthermore, GA-pre-treated mice showed restoration of alternation behavior and Aβ-induced memory impairment. We also found that GA inhibited NF-κB-mediated cytokine production in brain by blocking RelA acetylation. In summary, this study shows that selective modulation of NF-κB acetylation by a HATi is a potential mechanism for a new class of anti-neuroinflammatory or anti-neurodegenerative drugs.

2 Materials and methods

2.1 Cell culture and reagents

Murine BV-2 cells and Neuro-2A cells were obtained from the American Type Culture Collection (ATCC, Manassas, VA, USA; CRL Number: 2270). Fetal bovine serum (FBS), trypsin–EDTA, and penicillin–streptomycin were purchased from Gibco-BRL™ (Gaithersburg, MD, USA). 3-(4, 5-Dimethylthiazol-2-ly)-2,5-diphenyl tetrazolium bromide (MTT) was purchased from Sigma-Aldrich (St. Louis, MO, USA). $A\beta_{1-42}$ and $A\beta_{42-1}$ were purchased from BACHEM (Bubendorf, Switzerland). Other chemicals were purchased from Sigma-Aldrich.

BV-2 cells were cultured in DMEM (Gibco BRL) containing 5% heat-inactivated endotoxin-free FBS, 2 mM glutamine, 100 μg/mL streptomycin, and 100 U/mL penicillin in a humidified 5% CO_2 atmosphere at 37°C. Neuro-2A cells were

cultured in Modified Eagle's Medium (MEM; Gibco BRL) containing 10% heat-inactivated endotoxin-free FBS, 2 mM glutamine, 100 μg/mL streptomycin, and 100 U/mL penicillin in a humidified 5% CO_2 atmosphere at 37°C.

Primary glial cells were prepared from whole brains of postnatal day 1 Institute of Cancer Research (ICR) mice based on the method of Pan [21]. Briefly, dissected tissues were dissociated for 3 min with enzymatic digestion in 0.05% trypsin-EDTA and mechanically titrated in DMEM/F-12 without FBS. After centrifugation, the cells were plated on poly-L-lysine-coated 6-well or 10-cm plates in DMEM/F-12 medium with 10% FBS and 1% antibiotics. After 10–14 days in vitro, microglial cells were isolated from mixed glia by treatment with serum-free DMEM/F-12 medium and 0.25% trypsin-EDTA (4:1) for 30 min at 37°C. Non-adherent cells were removed by washing. Microglial cultures were used for experiments 1 DIV after isolation.

Aβ peptides were dissolved in PBS and pre-incubated at 37°C for 5 days to allow fibril formation. Peptides were stored at −20°C until use. GA was dissolved in DMSO and later diluted with distilled water (DMSO < 0.5% final concentration). For the co-culture experiments, BV-2 cells and primary microglial cells were treated with various concentrations of GA (5–50 μM final concentration) for 12 h prior to stimulation with aggregated $A\beta_{1-42}$ (5 μM; Aβ+GA group), $A\beta_{1-42}$ (5 μM), or medium only (control) for 24 h. Conditioned media (CM) from BV-2 cells and primary microglial cells were collected, centrifuged, and transferred to Neuro-2A cells for another 24 h. CM from the medium-only treated cells was used as a control. After incubation, cell viability was measured with the MTT assay, and western blotting was performed.

2.2 Cell viability assay (MTT assay)

Cell viability was measured to determine the cytotoxicity of Aβ peptides on microglial and neuronal cells. Cell viability was determined with the conventional MTT reduction assay. Briefly, microglial (BV-2) cells were seeded at 5×10^3–1×10^4 cells in a 96-well plate. After 12 h of incubation, cells were pre-incubated for 24 h with or without GA, and then cells were incubated with 1 μM $A\beta_{1-42}$ for another 24 h. Cells were then treated with 15 μL MTT solution (2 mg/mL) for 90 min at 37°C, the absorbance was recorded at 570 nm, and a reference was recorded at 630 nm with a micro plate reader (Model 550, BIO-RAD Laboratories, CA, USA). Also, Neuro-2A cells were seeded at 1×10^4–1×10^5 cells in a 96-well plate. After 12 h of incubation, medium was changed to CM from BV-2 and/or primary microglial cell cultures treated with or without β-amyloid and different concentrations of GA. Then, after 24 h of replacing the CM with non-CM, 15 μL MTT solution (2 mg/mL) was added for 90 min at 37°C, the absorbance was recorded at 570 nm, and a reference was recorded at 630 nm with a micro plate reader (Model 550, BIO-RAD).

2.3 Quantitative real-time RT-PCR analysis

Total RNA from Neuro-2A, BV-2, and primary microglial cells was extracted with TRIzol reagent (Invitrogen Life Technologies, Carlsbad, CA, USA) according to the manufacturer's instructions. The levels of iNOS, COX-2, and IL-1β mRNA were determined by QPCR (ABI PRISM 500 Sequence Detection System, Applied Biosystems, San Jose, CA, USA). cDNA amplification was performance in duplicate in 20-μL reaction mixtures containing 2× SYBR green master mix (Roche, Indianapolis, IN, USA) and 10 pM forward and reverse primers. The initial denaturation step was for 5 min at 95°C, followed by 40 amplification cycles: 30 s at 95°C, 30 s at 58°C, 30 s at 72°C, with a final 10-min extension at 72°C. Results were analyzed with ABI sequence detector software version 2.3. Relative mRNA expression of the target genes was calculated after normalizing to GAPDH expression and expressed as fold induction. The primers used in this study are listed in Table 1.

2.4 Subcellular fractionation

The cells were first resuspended in cold lysis buffer containing 10 mM Tris, pH 7.4, 10 mM KCl, 3 mM $MgCl_2$, 0.3% NP-40, and protease inhibitors and incubated for 20 min. Cytoplasmic proteins were separated by centrifugation. Then, extraction buffer containing 20 mM Tris buffer (pH 7.9), 420 mM NaCl, 0.2 mM EDTA, 10% glycerol, 2 mM DTT, and protease inhibitors was added to the cell pellet and incubated for an additional 20 min at 4°C. Lysates were then centrifuged at 20 000 × *g* for 20 min. Separated cytosolic proteins and nuclear proteins were stored at −70°C until immunoblotting.

2.5 Western Blotting

Treated cells were washed with cold PBS, scraped off, and harvested. Cells were then incubated for 20 min in lysis buffer containing 0.5% triton X-100, 20 mM HEPES (pH

Table 1. Primers

Name		Primer designs (5′ to 3′)
iNOS	Forward	TCTTGGAGCGAGTTGTGGAT
	Reverse	GGGTGGTAATGTCCAGGAAGT
COX-2	Forward	GAGTGGGAGGCACTTGCATT
	Reverse	TGGAGGCGAAGTGGGTTTTA
TNF-α	Forward	TTCTCATTCCTGCTTGTGGC
	Reverse	GTTTGCTACGACGTGGGCTA
IL-1β	Forward	GTTGACGGACCCCAAAAGAT
	Reverse	AAGGTCCACGGGAAAGACAC
GAPDH	Forward	GTGTTCCTACCCCCAATGTGT
	Reverse	AGGAGACAACCTGGTCCTCAGT

7.4), 150 mM NaCl, 2 mM DTT, and 1 mM PMSF. The lysates were centrifuged at 20 000 × *g* for 10 min at 4°C. The protein concentrations of clarified lysates were determined with the Bradford assay, with BSA as a reference. Total cell lysate protein was separated with 8 or 12% SDS-PAGE and transferred to nitrocellulose membranes. The membranes were blocked by incubating for 12 h in 5% w/v non-fat Difco™ skim milk blocking buffer. The blocked membranes were incubated overnight at 4°C with primary antibodies that recognize iNOS (1:1000), COX-2 (1:1000), IL-1β (1:500), NF-κB (p65; 1:500), acetyl-NF-κB (p65; 1:500), and β-actin (1: 5000). After extensive washing three times with PBS/0.1% Tween 20, the membranes were incubated with secondary horseradish peroxidase-conjugated antibody (1:1000) for 1 h. The bands were detected with the Enhanced Chemiluminescence System (Amersham Pharmacia Biotech) according to the manufacturer's instructions.

2.6 Immunohistochemistry

Mice were anesthetized and perfused transcardially with 0.9% saline, followed by chilled 4% paraformaldehyde in 0.1 M phosphate buffer, pH 7.4. Brains were removed and stored in fixative for 24 h and immersed in 30% sucrose solution in PBS for 72 h for the following studies. Brains were paraffin embedded, and 10-μm-thick sections were cut. The sections were incubated with rabbit polyclonal anti-IL-1β (1:500, Santa Cruz Biotechnology, Santa Cruz, CA, USA) and mouse monoclonal anti-NF-κB (p65; 1:500, Abcam, Cambridge, UK) followed by incubation with anti-rabbit (1:1000, Santa Cruz Biotechnology, Santa Cruz, CA, USA) and anti-mouse secondary antibodies (1:1000, Santa Cruz Biotechnology). The staining was visualized with a Vectastain ABC kit (Vector Laboratories, Burlingame, CA, USA). The stained sections were analyzed with a microscope (Carl Zeiss, Deutschland).

2.7 TUNEL assay

Based on a previous study [22], a TUNEL assay was performed with a kit (Roche, Nonnenwald, Germany) that detects double-stranded breaks in genomic DNA with diaminobenzidine. The treated cells were analyzed with a fluorescence microscope (Carl Zeiss).

2.8 Mouse experiment

Male ICR mice (Samtaco BioKorea, Korea) were used to measure cognitive function after a 1-wk adaptation period (20 to 22°C; 12-h light cycle from 09:00 to 21:00; feed, Agribrand Purina Korea, and water; both available ad libitum). The mice were divided into four groups ($n = 8$ each): the sham group, the Aβ-treated group, and groups co-treated with Aβ and GA (10 mg/kg B.W. or 30 mg/kg B.W.). Food and water were available ad libitum throughout the experiment. All experiments were conducted according to the guidelines of the Committee on Care and Use of Laboratory Animals of the Yonsei University. GA was dissolved in tap water at concentrations of 10 mg/kg and 30 mg/kg B.W. and orally administered for 28 days. After 21 days of treatment with GA, $A\beta_{1-42}$ and $A\beta_{42-1}$ were administered by intracerebroventricular (ICV) injection. Aβ peptides were dissolved in PBS and pre-incubated at 37°C for 5 days to allow fibril formation. The $A\beta_{1-42}$ injection was performed according to the procedure established by Chauhan et al. [28]. Briefly, a sterile saline (0.9% NaCl) containing Aβ1-42 was injected directly into the 3rd ventricle to be 0.25 mm posterior to the bregma of mice 2.5 depth (anteropoterior, −0.25 mm; mediolateral, 0 mm; dorsal ventral, 2.5 mm relative to the bregma).

After 26 days of treatment with GA, a Y-maze test was used to measure spatial working memory performance in mice with or without GA treatment by recording spontaneous alternation behavior. Each mouse, naive to the maze, was placed at the end of one arm and allowed to move freely through the maze during an 8-min session. The arm entries were recorded visually, and alternation was defined as successive entries into the three arms during non-overlapping triplet sets. The percentage alternation was calculated as the total number of arm entries minus two, multiplied by 100. Also, after 27 days of treatment with GA, the passive avoidance test was used to test learning and memory. A step-through type of passive avoidance test apparatus (Model PACS-30, Columbus Instruments Int., Columbus, OH, USA) was used to evaluate the effects of GA on learning and memory, essentially as described by Shen [29]. The shuttle box is divided into two chambers of equal size (23.5 × 15.5 × 15.5 cm), one illuminated and one dark, separated by a guillotine door. During the training trial, each mouse was placed in the lighted compartment, and when the mouse entered the dark compartment, the door was closed and the mouse received an inescapable electric shock (0.5 mA, 1 s). In the testing trial, given 1 day after the training trial, the mouse was again placed in the lighted compartment, and the latency time to enter the dark compartment was measured. If the mouse did not enter the dark chamber within the cut-off time (300 s), it was assigned a latency value of 300 s.

2.9 Preparation of tissue samples

After behavioral testing, mice were decapitated for western blotting. Brains were dissected and stored at −70°C until assessment. Brains were homogenized in ice-cold saline containing a protease inhibitor cocktail (Sigma-Aldrich). Homogenates were centrifuged at 10 000 rpm for 10 min, and the supernatant was used for western blotting.

2.10 Statistical analysis

All data are the mean ± SE. One-way analysis of variance was used to determine the effect of treatment. Differences among means were examined with Duncan's multiple range tests, and results were considered significant at a p-value of <0.05.

3 Results

3.1 GA prevents amyloid β-induced neuronal cell death by inhibiting RelA acetylation and cytokine production

First, we examined the effect of GA on cell viability with the MTT assay. In the result (Supporting information Fig. 1A, left panel), 5–50 μM GA treatment did not affect cell viability; however, a high concentration of GA (100 μM) was toxic to BV-2 and Neuro-2A cells. This result showed that the appropriate concentration of GA that did not induce cell toxicity was below 50 μM. Next, we examined the effect of Aβ-induced microglia activation on neuronal cell survival. For this experiment, CM from aggregated $A\beta_{1-42}$-treated microglial cells (Aβ-CM) were applied to Neuro-2A cells. Aβ treatment increased Neuro-2A cell death by approximately 50%; however, GA suppressed Aβ-induced neuronal cell death in a dose-dependent manner without affecting the survival of BV-2 cells (Fig. 1, right panel). These results showed the neuroprotective effect of GA. As a control, we found no apparent effect of Aβ-CM on BV-2 cell viability (Supporting information Fig. 1A, right panel). These results showed the neuroprotective effect of GA. Also, we found that effects of Aβ were less on cell viability of BV-2 than on that of Neuro-2A.

Because activated microglia-derived cytokines are responsible for neuronal cell death, we next examined whether GA suppressed cytokine production following Aβ-induced microglia activation. Upon Aβ treatment, cytokine production in both BV-2 cells and Aβ-CM-treated Neuro-2A cells was substantially increased (Supporting information Fig. 1B, left panel). As expected, GA treatment efficiently suppressed the expression of proinflammatory cytokines in a dose-dependent manner (Supporting information Fig. 1B, right panel). Consistent with this, western blot analysis showed a similar pattern as real-time PCR analysis (Supporting information Fig. 1C).

GA was recently shown to inhibit p300/CBP-mediated NF-κB acetylation and cytokine production [22]. Thus, we investigated whether GA inhibits Aβ-CM-induced NF-κB acetylation. As shown in Supporting information Fig. 1D, Aβ-CM treatment efficiently induced nuclear translocation of p65 and acetylation of p65; however, GA greatly reduced the levels of both nuclear p65 and p65 acetylation in Neuro-2A cells. These results indicated that GA prevented Aβ-induced cytokine production in BV-2 cells and Aβ-induced neuronal cell death by inhibiting p65 acetylation.

3.2 GA protects neuronal cells from primary microglia-mediated Aβ neurotoxicity

To consolidate our findings, we tested the neuroprotective effect of GA on primary microglia-mediated Aβ neurotoxicity. Similar to BV-2 cells, treatment with Aβ-CM from primary microglia reduced the cell viability of Neuro-2A cells, whereas GA reversed the Aβ-CM-mediated neuronal cell death in a dose-dependent manner (Fig. 1A). Both real-time PCR and western blot analysis demonstrated that GA consistently suppressed not only the Aβ-CM-induced cytokine production in Neuro-2A cells (Fig. 1C) but also Aβ-induced cytokine expression in primary microglia cells (Fig. 1B). In addition, GA treatment also efficiently suppressed the Aβ-CM-induced nuclear translocation of p65 as well as p65 acetylation (Fig. 1D). Collectively, our data showed that GA inhibited NF-κB acetylation, which suppressed Aβ-induced neuroinflammation and Aβ-mediated neurotoxicity.

3.3 GA treatment restores memory deficits in Aβ peptide-induced mice

Given the protective effects of GA in vitro, we next investigated the effects of GA in improving memory deficits in Aβ-treated mice. For this experiment, ICR mice were orally treated with 10 or 30 mg/kg B.W. GA for 28 days (Fig. 2A). All groups showed similar body weight changes following treatment with GA and Aβ peptide from the initial stage to the final stage (28 days; Table 2). For step-through latency (STL) with the passive avoidance paradigm, the Aβ-treated mice showed significantly shorter latency times during the retention trials, with a 63% decrease in STL compared to that of the normal controls. Mice given GA for 28 days prior to testing showed attenuation of Aβ-induced memory impairment. The STL decreased approximately 18 and 10% in the 10 and 30 mg/kg B.W. GA treatment groups, respectively, compared with the normal control group (Fig. 2B). Aβ peptide injection did not affect the general locomotor activities of the mice, but it led to learning and memory disabilities. However, treatment with GA ameliorated this cognitive dysfunction. The number of entries into the Y-maze was similar among the experimental groups (Fig. 2C). Only mice given Aβ peptide were impaired in spatial working memory as compared with the control group; however, pre-treatment with GA substantially reduced the effect of Aβ peptide on alternation behavior, by approximately 20% in the high-dose group compared to the Aβ-treated group (Fig. 2C). Therefore, these results confirmed the protective effects of GA on Aβ-induced cognitive dysfunction.

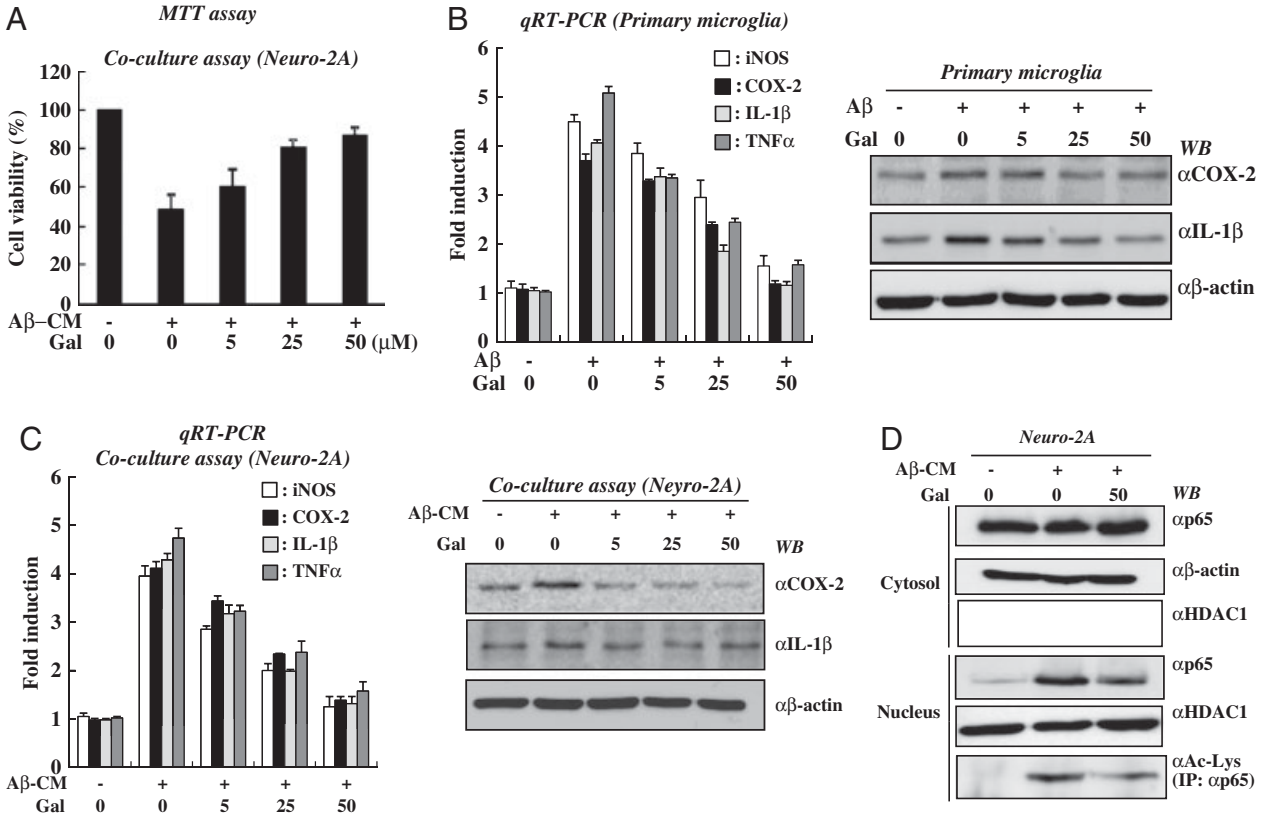

Figure 1. Inhibitory effect of GA on primary microglia-mediated Aβ neurotoxicity by blocking p65 acetylation. (A) The conditioned medium (CM) from primary microglia was transferred to Neuro-2A cells, and cell viability was assessed with the MTT assay. (B) The effect of GA on the expression of cytokines in primary microglia was analyzed with real-time PCR. Columns are the averages of three independent experiments; bars indicate the SD (left panel). The cytokine protein levels were analyzed with western blotting with the indicated antibodies (right panel). (C) The effect of GA on the expression of cytokines in Neuro-2A cells was analyzed with real-time PCR. Columns are the averages of three independent experiments; bars indicate the SD (left panel). The cytokine protein levels were analyzed with western blotting with the indicated antibodies (right panel). The CM from primary microglia was transferred to Neuro-2A cells. (D) Both nuclear and cytoplasmic extracts were prepared and immunoblotted with the indicated antibodies. To assess p65 acetylation, nuclear extracts were immunoprecipitated with the p65 antibody and immunoblotted with the acetyl-Lys antibody.

3.4 GA suppress in vivo cytokine production by inhibiting RelA acetylation in brain

Because GA efficiently reduced Aβ-induced memory impairment, we next examined whether GA suppressed the in vivo levels of $A\beta_{1-42}$-enhanced NF-κB acetylation and proinflammatory mediators. Oligomeric Aβ treatment greatly increased the levels of iNOS and COX-2 in cortex and hippocampus 5–10-fold compared with controls. On the other hand, pre-administration of GA (10 mg/kg B.W.) significantly inhibited the production of iNOS and COX-2 induced by Aβ peptide. In particular, treatment with 30 mg/kg B.W. GA completely restored the levels of both iNOS and COX-2 to levels similar to control levels in both cortex and hippocampus (Fig. 3A). Consistent with results from Qpcr analysis, western blotting analysis showed similar changes (Fig. 3B).

Because GA efficiently suppressed Aβ-induced cytokine production in both cortex and hippocampus, we then assessed the effect of pre-administered GA on the in vivo levels of NF-κB acetylation. As expected, pre-administration of GA dramatically inhibited the Aβ-enhanced production of iNOS and COX-2 in whole mouse brain (Fig. 3C). To measure the in vivo NF-κB acetylation level, whole brain lysates were immunoprecipitated with p65 antibody and immunoblotted with the acetylated lysine antibody. Aβ-treated mice showed increased levels of NF-κB acetylation. However, pre-administration of GA restored Aβ-enhanced NF-κB acetylation similar to control mice, showing the potent inhibitory effect of GA on in vivo NF-κB hyperacetylation. Interestingly, Aβ treatment had no effect on the level of NF-κB acetylation at Lys-310, which was previously shown to be a target of p300/CBP HAT, indicating that Aβ induced NF-κB acetylation on limited lysine residues rather than at all lysine residues in p65.

Finally, to solidify our findings, we assessed the level of nuclear NF-κB and IL-1β in mouse brain with immunohistochemistry. As shown in Fig. 3D, Aβ treatment greatly

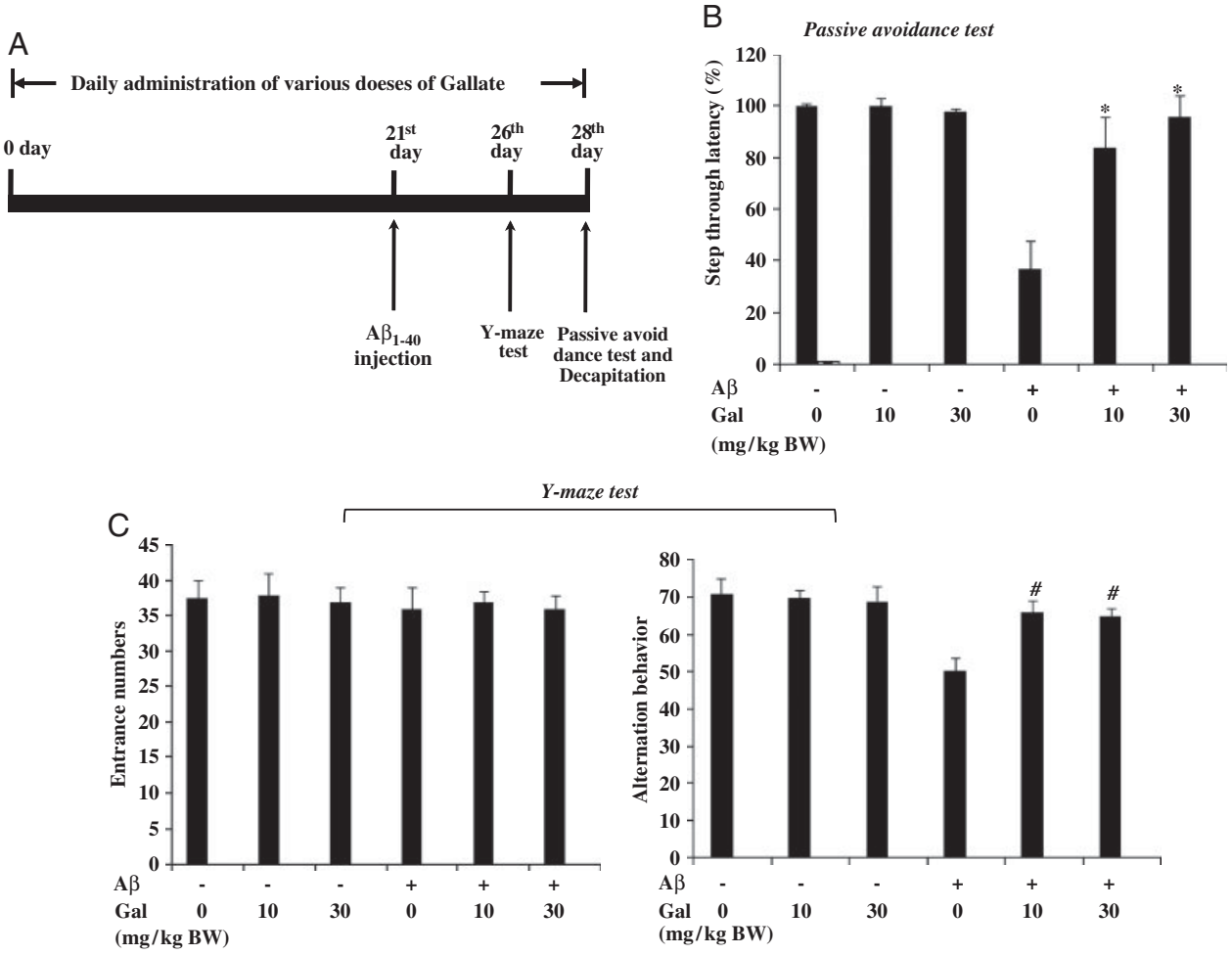

Figure 2. Effect of GA on cognitive functions in $A\beta_{1-42}$-injected mice. (A) Each behavioral test was conducted 5 days after $A\beta_{1-42}$ injection. GA was administered for 28 days (10 or 30 mg/kg B.W.). Aβ peptide was injected on day 21. (B) Passive avoidance was measured for 5 min in the shuttle box. (C) The number of arm entries and the spontaneous alternation behavior were measured during an 8-min session. The data are the mean ± SE ($n = 8$). A is non-significant. $^*p < 0.05$ versus only $A\beta_{42-1}$-injected group. sharp; $p < 0.05$ versus only $A\beta_{1-42}$-injected group.

Table 2. Effect of pre-administration of GA on weight changes over 28 days

Experimental group	Initial (g)	Final (g)
Control	21.0 ± 0.9	35.8 ± 0.6$^{N.S.}$
$A\beta_{1-42}$	20.2 ± 0.9	35.7 ± 0.6
$A\beta_{1-42}$ + 10 mg/kg B.W.	21.2 ± 0.4	36.6 ± 1.2
$A\beta_{1-42}$ + 30 mg/kg B.W.	20.9 ± 0.2	35.8 ± 0.5

Control mice were injected with $A\beta_{42-1}$. The data are the mean ± SE ($n = 10$). N.S.; not significant.

induced the nuclear translocation of NF-κB and the release of IL-1β in brain; however, pre-administration of GA substantially inhibited the increase in nuclear NF-κB and IL-1β. These results showed that GA suppressed the Aβ-induced cytokine release by inhibiting NF-κB acetylation in brain.

3.5 Pre-administration of GA protects neuronal cells from Aβ-induced neuronal cell death

To measure the protective effects of GA on Aβ-induced neuronal cell death, a TUNEL assay was performed in mouse brain. As shown in Fig. 4A, TUNEL-positive cells were found predominantly only in mice treated with Aβ peptide. Pre-administration of GA dramatically suppressed Aβ-mediated neuronal cell death, suggesting that GA protects neuronal cells from Aβ-induced neurotoxicity. Collectively, our results provide a possible therapeutic approach for using HATi such as GA for the effective

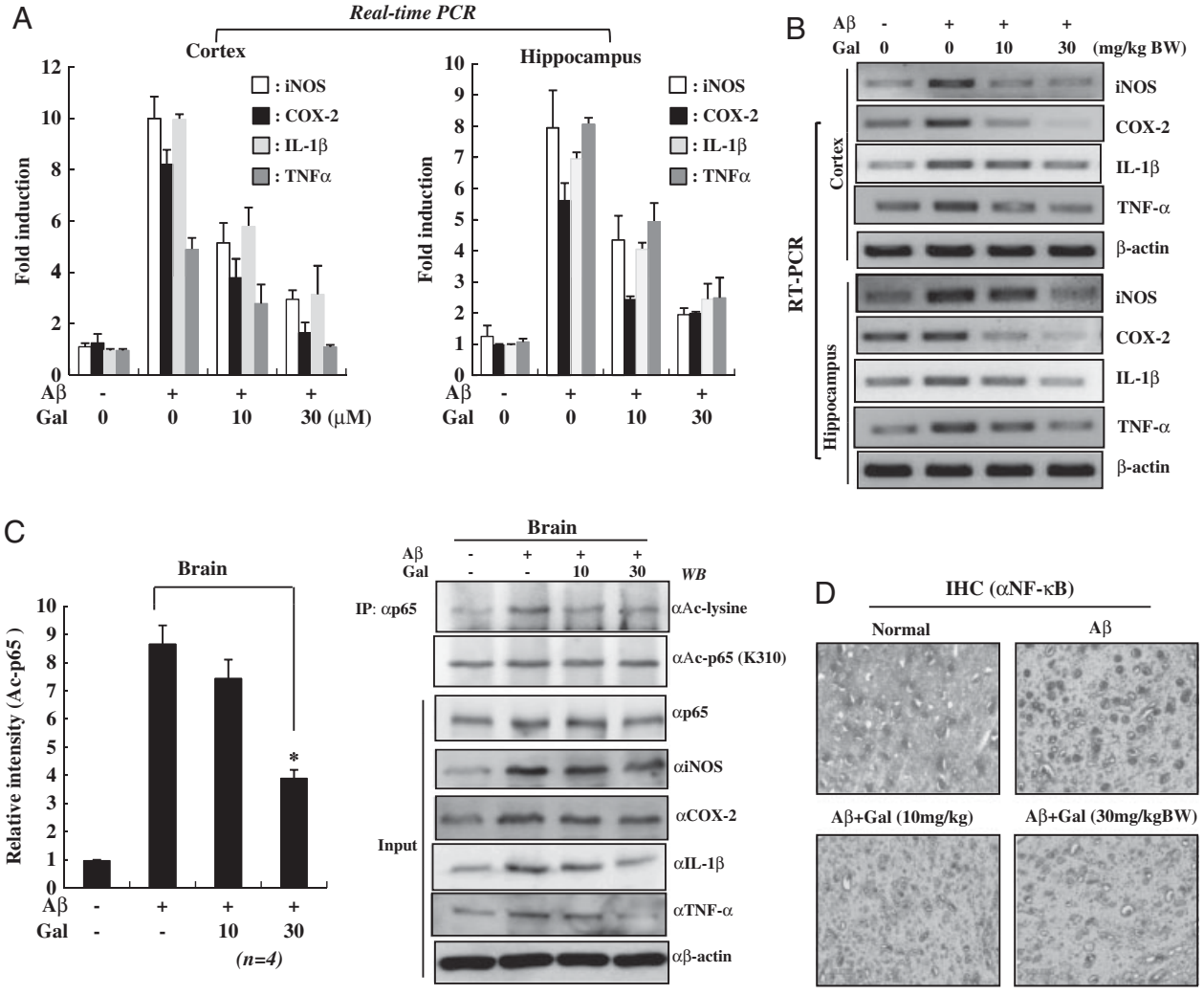

Figure 3. Effect of GA on in vivo cytokine production and RelA acetylation in brain. (A) Protein lysates were prepared from the hippocampus and cortex, and cytokine levels were analyzed with real-time PCR. (B) Western blot analysis was performed with indicated antibodies using the same batch of cells as for real-time PCR analysis. (C) Whole brain protein extract was analyzed with the indicated antibodies. To assess p65 acetylation, extracts were immunoprecipitated with the p65 antibody and immunoblotted with the acetyl-Lys antibody. Images were graphed using the Quantity one image program (Bio-rad). The data are the mean ± SE ($n = 4$). $^{*}p < 0.05$ versus only $A\beta_{1-42}$-injected group. (D) Both IL-1β and p65 expression were measured with immunohistochemistry in $A\beta_{1-42}$-injected whole mouse brain.

treatment of neuronal diseases by selectively blocking NF-κB-mediated microglial activation (Fig. 4B).

4 Discussion

NF-κB activation as a central event of inflammation is a common feature of many neurodegenerative diseases [18]. In the brains of patients with AD, NF-κB activation is observed predominantly in neurons and glial cells in areas surrounded by Aβ plaques [30, 31]. Furthermore, Aβ was also shown to activate NF-κB, which finally leads to increased cytokine production in neurons and glial cells [32]. In this regard, non-steroidal anti-inflammatory drugs (NSAIDs) such as flurbiprofen have been shown to effectively reduce the formation of Aβ plaques by directly inhibiting NF-κB in AβPP transgenic mice [33, 34] or by direct modulation of γ-secretase [33, 35]. Therefore, effective inhibition of NF-κB activation may be one of the useful ways to block Aβ-induced neuroinflammation in patients with AD.

It has been reported that HAT enzyme-mediated NF-κB acetylation is required for the nuclear translocation and subsequent activation of NF-κB signaling [12]. Thus, HAT-mediated NF-κB hyperacetylation is believed to be a critical step in the NF-κB-mediated inflammatory response, which is presumably correlated with the development of many pathological states, especially those involving acute inflammation

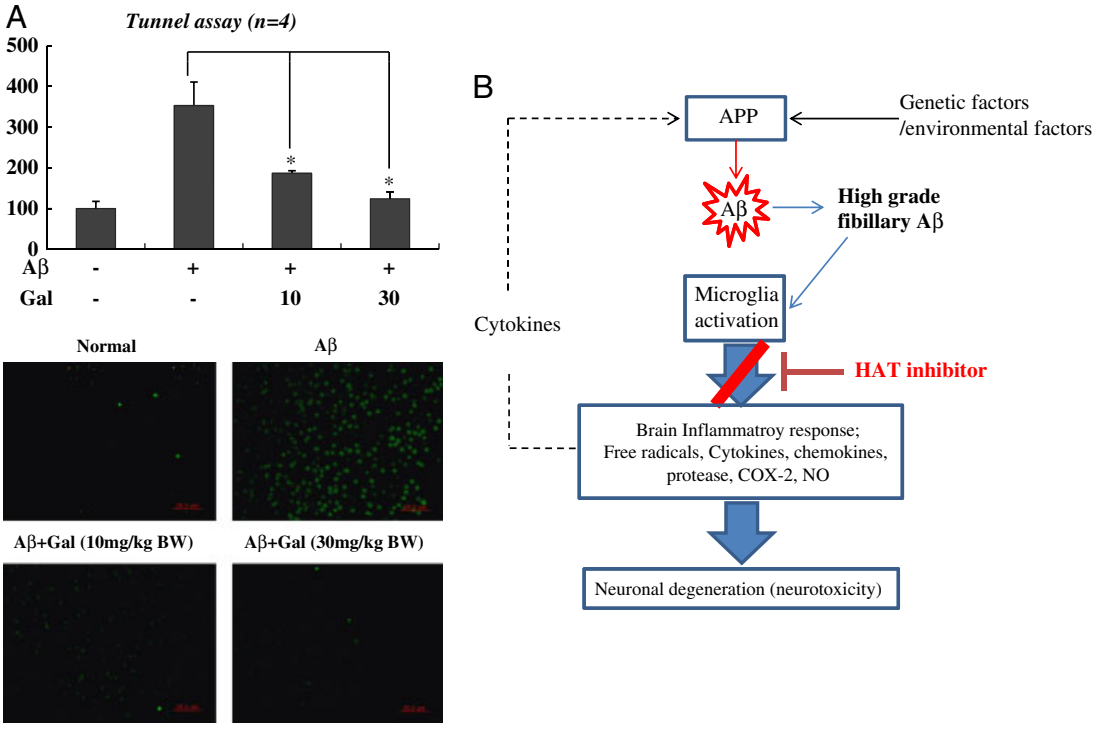

Figure 4. Effect of GA on neuronal cell death in $A\beta_{1-42}$-injected mouse brain. (A) Cell viability in $A\beta_{1-42}$-injected mouse brain was assessed with the TUNEL assay. The data are the mean ± SE ($n = 4$). $^{*}p < 0.05$ versus only $A\beta_{1-42}$-injected group. (B) Models of our findings. Aβ peptide-activated microglia show increased expression of cytokines such as iNOS, COX-2, and IL-1β via NF-κB hyperacetylation. Then, activated microglia mediate Aβ neurotoxicity. However, blocking NF-κB acetylation by HATi inhibits NF-κB-mediated neuroinflammatory signaling and consequent activation of microglia, which may prevent neuronal cell death.

such as in AD. In this study, we propose a possible therapeutic approach using HATi to alleviate neuroinflammation-induced neurotoxicity. Our group recently identified GA as a potent HATi with a broad spectrum of enzyme specificity [22]. In addition, we also showed that GA inhibits LPS-induced NF-κB acetylation and cytokine production in vitro and in vivo. Based on this finding, we have examined whether GA suppresses oligomeric Aβ-induced NF-κB acetylation and cytokine production. As shown in vitro and in vivo, GA treatment efficiently restored the Aβ-mediated NF-κB activation and enhanced production of cytokines. In particular, we showed that pre-administration of GA greatly suppressed in vivo NF-κB acetylation and Aβ-mediated neurotoxicity. Therefore, our study suggests a possible use for HATi in blocking neuroinflammation.

Without direct observation of GA permeability into BBB, We predict the brain availabilty of GA based on the physical property of Log*p* value. Log*p* value is important to judge the lipophilicity of a compound and can be used as a parameter for the BBB permeability. The reported optimal Log*p* values are in the 1.5–2.7 for BBB penetration [36] and GA is 0.89. Although the lipophilicity of GA is lower than the optimal values, the value is close to the optimal condition. Therefore, we presume that certain level of used GA can be available in the brain.

Two HAT enzymes, p300/CBP and PCAF, are known to acetylate the lysine residues of NF-κB (RelA) [12]. p300/CBP was shown to acetylate the majority of lysine residues in the NF-κB protein [12]. In contrast, PCAF specifically acetylates Lys-122 of NF-κB. Acetylation of Lys-310, which is mediated by p300/CBP, is a hallmark of the nuclear translocation of NF-κB and subsequent NF-κB activation [21]. Thus, we initially expected that Aβ treatment would induce acetylation of Lys-310 in NF-κB. However, the Aβ-dependent increase in NF-κB acetylation was only detected with a Lys-specific antibody but not with an antibody against acetylated NF-κB (Lys-310; data not shown). This observation suggested the possible involvement of PCAF in Aβ-induced NF-κB activation instead of p300/CBP. Importantly, recent studies using PCAF knock-out mice have demonstrated that Aβ treatment fails to induce memory deficits and neuronal cell death when PCAF is depleted, indicating a critical role for PCAF in Aβ-induced cognitive dysfunction [37, 38]. In addition, microarray expression data analysis with the Human BLAT Search database (http://genome.ucsc.edu) showed predominant expression of Pcaf in brain compared to p300/CBP (Supporting Information Figure 2), implying a critical role for PCAF in neuroinflammation. Because GA is known to inhibit the activity of PCAF as well as p300/CBP, it is possible that GA suppresses Aβ-induced NF-κB

acetylation by inhibiting PCAF. Future studies examining the roles of PCAF in neuroinflammation will be interesting.

In summary, we found that GA treatment suppressed Aβ-induced NF-κB activation and production of cytokines in microglial cells via RelA hypoacetylation, which finally led to the reduction of Aβ-induced neurotoxicity. We also showed a restorative effect of GA on Aβ-induced cognitive dysfunction. Finally, we found that GA treatment efficiently blocked neuronal cell death by downregulating the expression of cytokines and the in vivo level of NF-κB acetylation.

Collectively, our results suggest that selective inhibition of NF-κB acetylation by HATi is a possible therapeutic approach for alleviating the progression of AD.

This study was supported by a grant from the Korea Health Care Technology R&D Project, Ministry for Health, Welfare & Family Affairs, Republic of Korea (A092039) and by the National Research Foundation of Korea (NRF) grant funded by the Korea Government (MEST) (No. 2011-0030709). Mi-Jeong Kim and Ah-Reum Seong contributed equally to this work.

The authors have declared no conflict of interest.

5 References

[1] Mattson, M. P., Apoptosis in neurodegenerative disorders. *Nat. Rev. Mol. Cell. Biol.* 2000, *1*, 120–129.

[2] Citron, M., Alzheimer's disease: treatments in discovery and development. *Nat. Neurosci.* 2002, *5*, 1055–1057.

[3] Dheen, S. T., Kaur, C., Ling, E. A., Microglial activation and its implications in the brain diseases. *Curr. Med. Chem.* 2007, *14*, 1189–1197.

[4] Graeber, M. B., Streit, W. J., Microglia: biology and pathology. *Acta Neuropathol.* 2010, *119*, 89–105.

[5] Bonaiuto, C., McDonald, P. P., Rossi, F., Cassatella, M. A., Activation of nuclear factor-kappa B by beta-amyloid peptides and interferon-gamma in murine microglia. *J. Neuroimmunol.* 1997, *77*, 51–56.

[6] Kim, S. H., Smith, C. J., Van Eldik, L. J., Importance of MAPK pathways for microglial pro-inflammatory cytokine IL-1 beta production. *Neurobiol. Aging* 2004, *25*, 431–439.

[7] Qiu, D., Zhao, G., Aoki, Y., Shi, L. et al., Immunosuppressant PG490 (triptolide) inhibits T-cell interleukin-2 expression at the level of purine-box/nuclear factor of activated T-cells and NF-kappaB transcriptional activation. *J. Biol. Chem.* 1999, *274*, 13443–13450.

[8] Pahl, H. L., Activators and target genes of Rel/NF-kappaB transcription factors. *Oncogene* 1999, *18*, 6853–6866.

[9] Baldwin, A. S., Jr., The NF-kappa B and I kappa B proteins: new discoveries and insights. *Annu. Rev. Immunol.* 1996, *14*, 649–683.

[10] Ghosh, S., May, M. J., Kopp, E. B., NF-kappa B and Rel proteins: evolutionarily conserved mediators of immune responses. *Annu. Rev. Immunol.* 1998, *16*, 225–260.

[11] Jobin, C., Morteau, O., Han, D. S., Balfour Sartor, R., Specific NF-kappaB blockade selectively inhibits tumour necrosis factor-alpha-induced COX-2 but not constitutive COX-1 gene expression in HT-29 cells. *Immunology* 1998, *95*, 537–543.

[12] Chen, L. F., Mu, Y., Greene, W. C., Acetylation of RelA at discrete sites regulates distinct nuclear functions of NF-kappaB. *EMBO J.* 2002, *21*, 6539–6548.

[13] Kiernan, R., Bres, V., Ng, R. W., Coudart, M. P. et al., Post-activation turn-off of NF-kappa B-dependent transcription is regulated by acetylation of p65. *J. Biol. Chem.* 2003, *278*, 2758–2766.

[14] Viatour, P., Legrand-Poels, S., van Lint, C., Warnier, M. et al., Cytoplasmic IkappaBalpha increases NF-kappaB-independent transcription through binding to histone deacetylase (HDAC) 1 and HDAC3. *J. Biol. Chem.* 2003, *278*, 46541–46548.

[15] Hayden, M. S., Ghosh, S., Signaling to NF-kappaB. *Genes Dev.* 2004, *18*, 2195–2224.

[16] Shishodia, S., Aggarwal, B. B., Nuclear factor-kappaB activation: a question of life or death. *J. Biochem. Mol. Biol.* 2002, *35*, 28–40.

[17] Chen, J., Zhou, Y., Mueller-Steiner, S., Chen, L. F. et al., SIRT1 protects against microglia-dependent amyloid-beta toxicity through inhibiting NF-kappaB signaling. *J. Biol. Chem.* 2005, *280*, 40364–40374.

[18] Kaltschmidt, B., Uherek, M., Volk, B., Baeuerle, P. A., Kaltschmidt, C., Transcription factor NF-kappaB is activated in primary neurons by amyloid beta peptides and in neurons surrounding early plaques from patients with Alzheimer disease. *Proc. Natl. Acad. Sci. USA* 1997, *94*, 2642–2647.

[19] Sung, B., Pandey, M. K., Ahn, K. S., Yi, T. et al., Anacardic acid (6-nonadecyl salicylic acid), an inhibitor of histone acetyltransferase, suppresses expression of nuclear factor-kappaB-regulated gene products involved in cell survival, proliferation, invasion, and inflammation through inhibition of the inhibitory subunit of nuclear factor-kappaBalpha kinase, leading to potentiation of apoptosis. *Blood* 2008, *111*, 4880–4891.

[20] Morimoto, T., Sunagawa, Y., Kawamura, T., Takaya, T. et al., The dietary compound curcumin inhibits p300 histone acetyltransferase activity and prevents heart failure in rats. *J. Clin. Invest.* 2008, *118*, 868–878.

[21] Choi, K. C., Jung, M. G., Lee, Y. H., Yoon, J. C. et al., Epigallocatechin-3-gallate, a histone acetyltransferase inhibitor, inhibits EBV-induced B lymphocyte transformation via suppression of RelA acetylation. *Cancer Res.* 2009, *69*, 583–592.

[22] Choi, K. C., Lee, Y. H., Jung, M. G., Kwon, S. H. et al., Gallic acid suppresses lipopolysaccharide-induced nuclear factor-kappaB signaling by preventing RelA acetylation in A549 lung cancer cells. *Mol. Cancer Res.* 2009, *7*, 2011–2021.

[23] Balasubramanyam, K., Altaf, M., Varier, R. A., Swaminathan, V. et al., Polyisoprenylated benzophenone, garcinol, a natural histone acetyltransferase inhibitor, represses chromatin transcription and alters global gene expression. *J. Biol. Chem.* 2004, *279*, 33716–33726.

[24] Negi, A. S., Darokar, M. P., Chattopadhyay, S. K., Garg, A. et al., Synthesis of a novel plant growth promoter from gallic acid. *Bioorg. Med. Chem. Lett.* 2005, *15*, 1243–1247.

[25] Yoshiki, Y., Kahara, T., Okubo, K., Sakabe, T., Yamasaki, T., Superoxide- and 1,1-diphenyl-2-picrylhydrazyl radical-scavenging activities of soyasaponin beta g related to gallic acid. *Biosci. Biotechnol. Biochem.* 2001, *65*, 2162–2165.

[26] Kubo, I., Xiao, P., Fujita, K., Antifungal activity of octyl gallate: structural criteria and mode of action. *Bioorg. Med. Chem. Lett.* 2001, *11*, 347–350.

[27] Wang, Y. J., Thomas, P., Zhong, J. H., Bi, F. F. et al., Consumption of grape seed extract prevents amyloid-beta deposition and attenuates inflammation in brain of an Alzheimer's disease mouse. *Neurotox. Res.* 2009, *15*, 3–14.

[28] Chauchan, N. B., Siegel, G. J., Lichtor, T., Distribution of intraventriculary administrated antiamyloid-β peptide(Aβ) antibody in the mouse brain. *J. Neurosci. Res.* 2001, *66*, 31–235.

[29] Shen, Z., Wang, G., Lin, S. Z., Two-way shuttlebox avoidance conditioning and brain NADH in rats. *Physiol. Behav.* 1990, *48*, 515–517.

[30] Boissiere, F., Hunot, S., Faucheux, B., Duyckaerts, C. et al., Nuclear translocation of NF-kappaB in cholinergic neurons of patients with Alzheimer's disease. *Neuroreport* 1997, *8*, 2849–2852.

[31] Lukiw, W. J., Bazan, N. G., Strong nuclear factor-kappaB-DNA binding parallels cyclooxygenase-2 gene transcription in aging and in sporadic Alzheimer's disease superior temporal lobe neocortex. *J. Neurosci. Res.* 1998, *53*, 583–592.

[32] Akama, K. T., Albanese, C., Pestell, R. G., Van Eldik, L. J., Amyloid beta-peptide stimulates nitric oxide production in astrocytes through an NFkappaB-dependent mechanism. *Proc. Natl. Acad. Sci. USA* 1998, *95*, 5795–5800.

[33] Eriksen, J. L., Sagi, S. A., Smith, T. E., Weggen, S. et al., NSAIDs and enantiomers of flurbiprofen target gamma-secretase and lower Abeta 42 in vivo. *J. Clin. Invest.* 2003, *112*, 440–449.

[34] Sung, S., Yang, H., Uryu, K., Lee, E. B. et al., Modulation of nuclear factor-kappa B activity by indomethacin influences A beta levels but not A beta precursor protein metabolism in a model of Alzheimer's disease. *Am. J. Pathol.* 2004, *165*, 2197–2206.

[35] Weggen, S., Eriksen, J., Das, P., Sagi, S. et al., A subset of NSAIDs lower amyloidogenic Abeta42 independently of cyclooxygenase activity. *Nature* 2001, *414*, 212–216.

[36] Pajouhesh, H., Lenz, G., Medicinal chemical properties of successful central nervous system drugs. *NeuroRx* 2005, *2*, 541–553.

[37] Duclot, F., Meffre, J., Jacquet, C., Gongora, C., Maurice, T., Mice knock out for the histone acetyltransferase p300/CREB binding protein-associated factor develop a resistance to amyloid toxicity. *Neuroscience* 2010, *167*, 850–863.

[38] Maurice, T., Duclot, F., Meunier, J., Naert, G. et al., Altered memory capacities and response to stress in p300/CBP-associated factor (PCAF) histone acetylase knockout mice. *Neuropsychopharmacology* 2008, *33*, 1584–1602.

